Electronic Supplementary Material (ESI) for Journal of Materials Chemistry B.

Glycopolymer Decorated Multiwall Carbon Nanotubes for Dual Targeted Breast Cancer Therapy

Pinar Sinem Omurtag Ozgen*[a], Sezen Atasoy[b], Belma Zengin Kurt[c], Zehra Durmus[d], Gulsah Yigit[e], Aydan Dag*[c,f]

[a]Department of Analytical Chemistry, Faculty of Pharmacy, Istanbul Medipol University, 34815, Istanbul, Turkey

[b]Department of Biochemistry, Faculty of Pharmacy, Bezmialem Vakif University, 34093, Istanbul, Turkey

[c]Department of Pharmaceutical Chemistry, Faculty of Pharmacy, Bezmialem Vakif University, 34093, Istanbul, Turkey

[d]Baglar Mah., Gunesli Konutlar, No: 38, D-24, 34212, Istanbul, Turkey

[e]Department of Biotechnology, Institute of Health Sciences, Bezmialem Vakif University, 34093, Istanbul, Turkey

[f]Drug Application and Research Center, Bezmialem Vakif University, 34093, Istanbul, Turkey

Table of Contents

3. Supplementary Figures

Figure S1. ^{1}H-NMR spectrum of 4-cyanopentanoic acid dithiobenzoate (CPADB) in $CDCl_3$ (500 MHz).

Figure S 2. ^{13}C-NMR spectrum of 4-cyanopentanoic acid dithiobenzoate(CPADB) in $CDCl_3$(125 MHz).

Figure S3. ^{1}H-NMR spectrum of Pyren-1-ylmethyl 4-cyano-4-((phenylcarbonothioyl)thio) pentanoate (CPADB-Py) in $CDCl_3$ (500 MHz).

Figure S4. ^{13}C-NMR spectrum of Pyren-1-ylmethyl 4-cyano-4-((phenylcarbonothioyl)thio) pentanoate (CPADB-Py) in $CDCl_3$ (125 MHz).

Figure S5. FT-IR spectrum of pyren-1-ylmethyl 4-cyano-4-((phenylcarbonothioyl)thio) pentanoate.

Figure S6. ^{1}H-NMR spectrum of 3-azidopropanoic acid (1) in $CDCl_3$ (500 MHz).

Figure S7. ^{1}H-NMR spectrum of 2-azidoethyl 4-cyano-4-((phenylcarbonothioyl)thio) pentanoate (CPADB-N_3) in $CDCl_3$ (500 MHz).

Figure S8. ^{13}C-NMR spectrum of 2-azidoethyl 4-cyano-4-((phenylcarbonothioyl)thio) pentanoate (CPADB-N_3) in $CDCl_3$ (125 MHz).

Figure S9. FT-IR spectrum of 2-azidoethyl4-cyano-4-((phenylcarbonothioyl)thio)pentanoate.

Figure S10. ^{1}H-NMR spectrum of *p*-(2-hydroxyethoxy)benzaldehyde (PEHBA) in $CDCl_3$ (500 MHz).

Figure S11. ^{1}-H NMR spectrum of p-(2-methacryloxyethoxy)benzaldehyde in $CDCl_3$ (500 MHz).

Figure S12. ^{13}C NMR spectrum of *p*-(2-methacryloxyethoxy)benzaldehyde in $CDCl_3$ (125 MHz).

Figure S13. FT-IR spectrum of *p*-(2-methacryloxyethoxy)benzaldehyde (MAEBA).

Figure S 14. ^{1}H-NMR spectrum of 2,3:4,5 di-*O*-isopropylidene β-D-fructopyranose in $CDCl_3$ (500 MHz).

Figure S15. FT-IR spectra of D-Fructose (black), 2,3:4,5 di-*O*-isopropylidene β-D-fructopyranose and 1-*O*-methacryloyl 2,3:4,5-di-*O*-isopropylidene-β-D-fructopyranose.

Figure S16. ^{1}H-NMR spectrum of 1-*O*-methacryloyl 2,3:4,5-di-*O*-isopropylidene-β-D-fructopyranose in $CDCl_3$ (500 MHz).

Figure S17. ^{13}C-NMR spectrum of 1-*O*-methacryloyl 2,3:4,5-di-*O*-isopropylidene-β-D-fructopyranose in $CDCl_3$ (125 MHz).

Figure S18. ^{1}H-NMR spectrum of P(MAEBA)-Py (**P1**) in $CDCl_3$ (500 MHz).

Figure S19. ^{1}H-NMR spectrum of P(*ip*FruMA-*b*-MAEBA)-Py (**P3**) in $CDCl_3$ (500 MHz).

Figure S20. ^{1}H-NMR spectrum of P(FruMA-*b*-MAEBA)-Py (**P5**) in DMSO-d_6 (500 MHz).

Figure S21. A) UV spectra of **P1, P3, P5** and **P7 B)** FT-IR spectra of **P1**, **P3** and **P7**.

1. Materials

All materials were reagent grade and used as received, unless otherwise specified:

1-pyrenemethanol (98%), 4-(dimethylamino) pyridine (DMAP, purum, ≥98.0%), dicyclohexylcarbodiimide (DCC, 99%), 2-bromoethanol (95%), sodium azide (≥99%, ultradry), 4-hydroxy benzaldehyde (98%), triethylamine (Et_3N, ≥99%), D-Fructose (≥99%), tetrahydrofuran (THF, for analysis EMSURE® ACS,Reag. Ph Eur), toluene (for analysis EMSURE® ACS,ISO,Reag. Ph Eur) and *N*,*N*-dimethylformamide (DMF, ≥99.8%) were all from Sigma-Aldrich.

2,2′-Azobis(2-methylpropionitrile) (AIBN, Sigma-Aldrich) was recrystallized twice from methanol (MeOH) and stored at −18 °C.

Ethyl acetate (EtOAc, ≥99.7% LC-MS), hexane (for Liquid Chromatography) and dimethylsulfoxide (DMSO; for analysis ACS) were purchased from ISOLAB chemicals

Ethanol (EMSURE® Reag. Ph Eur, 96%), acetonitrile (for liquid chromatography LiChrosolv® Reag. Ph Eur) were purchased from Merck.

Ultrapure (UP) water was produced by a Milli-Q reverse osmosis system and had a resistivity of 19.6 MΩ·cm.

Dulbecco's modified eagle medium: nutrient mixture F-12 (DMEM/F12), Fetal bovine serum (FBS), Penicillin-Streptomycin, Trypsin-ethylene diamine tetra acetic acid (EDTA), phosphate buffered saline (PBS) were all from Gibco, Thermo Fisher Scientific, MA, USA. T flasks, 96-well plates, and cell culture supplies were purchased from Isolab GmbH, Germany.

3-(4,5-dimethylthiazol-2-yl)-2,5-diphenyltetrazolium bromide (MTT), 4',6-diamidino-2-phenylindole (DAPI) were from Invitrogen, Thermo Fisher Scientific, MA, USA.

Muse™ Annexin V & Dead Cell Reagent and Muse™ Cell Cycle Reagent were purchased from Merck-Millipore (Darmstadt, Germany) Hoechst 33342 were from Cell Signaling Technology (MA, USA).

2. Characterization

Gel Permeation Chromatography (GPC)

The molecular weight and polydispersity of synthesized polymers were analyzed via gel permeation chromatography (GPC). A Viscotek GPCmax modular system comprising a VE 2001 autoinjector, Viscotek VE 3580 refractive index (RI) detector was used. A Viscotek CLM3008 guard column (4.6 × 10 mm) followed by three 300 × 7.8 mm linear columns (T3000, LT4000L, and LT5000L), (7.8x 300 mm) were employed for analysis. Tetrahydrofuran (THF, HPLC grade, 0.05% w/v 2,6-dibutyl-4-methylphenol (BHT)) with a flow rate of 1 mL/min at 35 °C was used as mobile phase. Fifty microliters of polymer solution sample with a concentration of 4-5 mg/ mL in THF was used for every injection. The calibration was performed using commercially available narrow-polydispersity polystyrene (PS) standards (Polymer Laboratories). DMF-GPC experiments were performed on a TOSOH EcoSEC/GPC system equipped with a refractive index (RI) detector, a UV detector, a DLS Wyatt Dynapro Nanostar detector and a DAWN HELEOS-18 multi-angle laser light scattering detector, (MALLS detector, Wyatt Technology, Santa Barbara, CA, USA). N,N-Dimethylformamide (0.01 M LiBr/DMF, HPLC grade DMF) with a flow rate of 0.5 mL/min at 45 °C was used as the mobile phase. DMF-GPC analyses were performed using serially connected size-exclusion columns (TSKgel HHR guard column, G3000 HHR and G5000 HHR (7.8 mm ID x 30 cm)).

Nuclear Magnetic Resonance (NMR) Spectroscopy

NMR general characterization was conducted using a Bruker BioSpin AG Avance 500 mHz Spectrometer (^{1}H (500 MHz), ^{13}C (125 MHz)). Samples were analyzed in the solvents of $CDCl_3$ and DMSO-d_6. All chemical shifts are stated in ppm (δ) relative to $Si(CH_3)_4$ as internal standard (δ = 0 ppm), referenced to the chemical shifts of residual solvent resonances (^{1}H and ^{13}C).

Fourier-Transform Infrared (FT-IR) Spectroscopy

A Bruker Alpha infrared spectrometer equipped with an attenuated total reflectance (ATR) device and germanium crystal was used. FT-IR spectra of samples were recorded within a wave number range of 400-4000 cm^{-1} with a resolution of 4 cm-1 from 16 scans in transmission mode. The spectra were analyzed by using the "OPUS" and Origin v8.5 software.

Dynamic Light Scattering Measurements (DLS)

Nanoparticle sizes (the average hydrodynamic diameters and size distributions of the prepared nanoparticle solutions) were determined using a Malvern Zetasizer Nano ZS particle size analyzer equipped with a 4 mV He-Ne laser operating at $\lambda = 632$ nm, an avalanche photodiode detector with high quantum efficiency, and an ALV/LSE-5003 multiple tau digital correlator electronics system. Samples were prepared at a polymer concentration of 1 mg/ mL in UP water and purified from dust using a microfilter (0.45 μm) prior to the measurements.

Thermal Gravimetric Analysis (TGA)

The thermal stability was determined by thermogravimetric analysis (TGA) with a Perkin Elmer Instruments model, TGA 8000 for 5 mg of powder sample at a heating rate of 10 °C per min.

Differential Scanning Calorimetry (DSC)

Differential scanning calorimetry (DSC) measurements were performed on a TA Instruments Discovery DSC 250 with a heating rate of 10 °C min^{-1} under nitrogen atmosphere. The masses of the dried samples were approximately 1-1.5 mg.

Transmission Electron Microscope (TEM)

The TEM micrographs were obtained using a Hitachi HT7800 transmission electron microscope. The instrument operates at an accelerating voltage of 200 kV. Samples were imaged without any staining. The particles were cast onto a carbon-coated copper grid by

placing a droplet a micelle aqueous solution for 15 min onto its surface. Subsequently, the excess of the solution was removed using filter paper. The grids were dried on air.

In vitro Drug Release Profile of Doxorubicin (Dox) from CNT/P7

The release rate of Dox from CNT/P7 was evaluated by the dialysis method in two different pH buffer solutions (pH= 5.5 and pH 7.4). CNT/P7 was dispersed in 2.5 mL of pH buffer solution and then placed into a dialysis cell with a molecular weight cutoff of 3500 Da. CNT/P7 was dialyzed against 80 mL of phosphate buffered saline (PBS) containing (10 mM) 150 mM NaCl at slightly alkaline and endosomal pH (pH 5.5) in physiological conditions in a thermo-controlled shaker with a stirring speed of 120 rpm at 37 °C. The 3 mL of samples were taken from the dialysis medium at a certain time point for UV-Vis measurement and were replaced in the same volume of the fresh media. The quantity of drug released into the media at each time interval was calculated as the percentage of total drug released to the initial amount of the drug. This process was performed with three replicates. It is shown in Electronic Supplementary (ESI) Figure S33.

3. Supplementary Figures

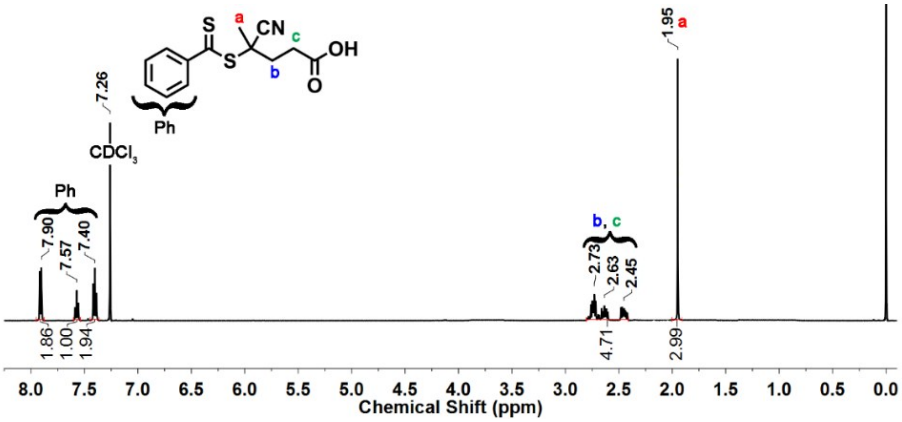

Figure S1. ^{1}H-NMR spectrum of 4-cyanopentanoic acid dithiobenzoate (CPADB) in $CDCl_3$ (500 MHz).

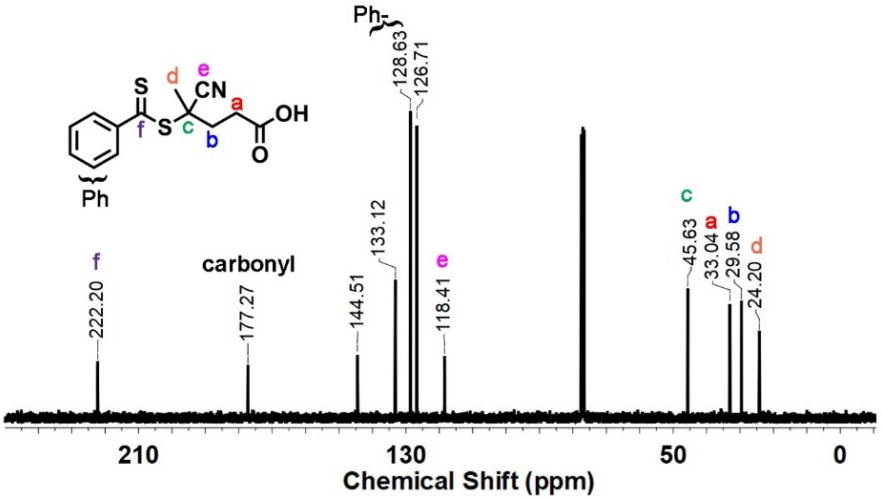

Figure S2. ^{13}C-NMR spectrum of 4-cyanopentanoic acid dithiobenzoate (CPADB) in $CDCl_3$ (125 MHz).

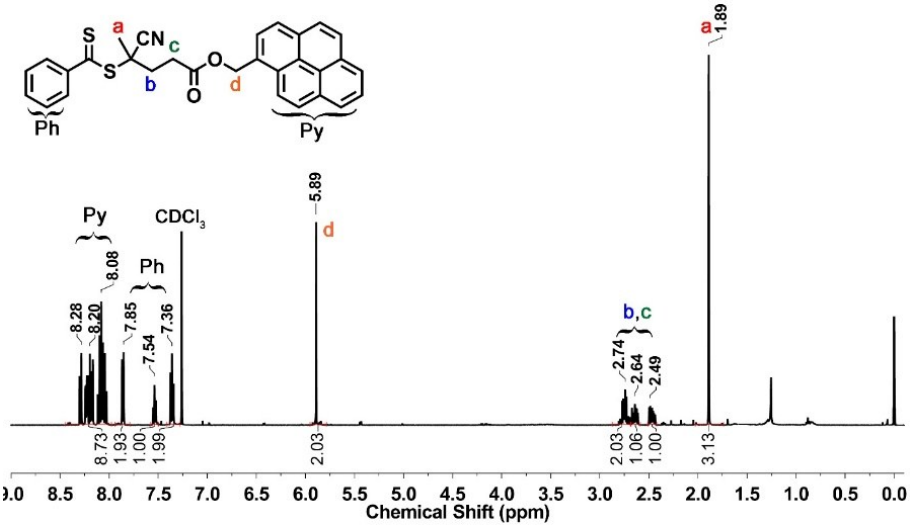

Figure S3. ^{1}H-NMR spectrum of Pyren-1-ylmethyl 4-cyano-4-((phenylcarbonothioyl)thio) pentanoate (CPADB-Py) in $CDCl_3$ (500 MHz).

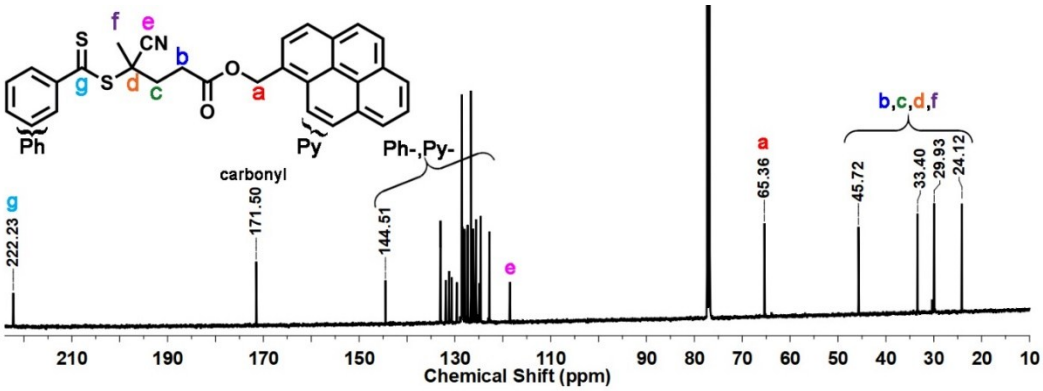

Figure S4. ^{13}C-NMR spectrum of Pyren-1-ylmethyl 4-cyano-4-((phenylcarbonothioyl)thio) pentanoate (CPADB-Py) in $CDCl_3$ (125 MHz).

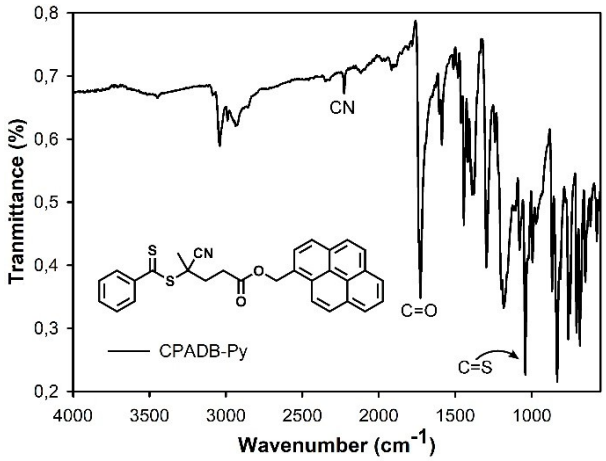

Figure S5. FT-IR spectrum of pyren-1-ylmethyl 4-cyano-4-((phenylcarbonothioyl)thio) pentanoate (CPADB-Py).

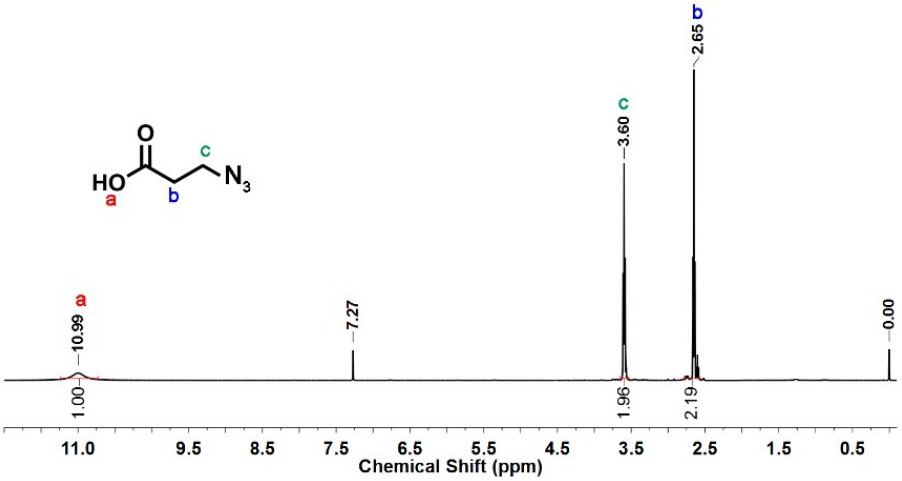

Figure S6. ^{1}H-NMR spectrum of 3-azidopropanoic acid (1) in $CDCl_3$ (500 MHz).

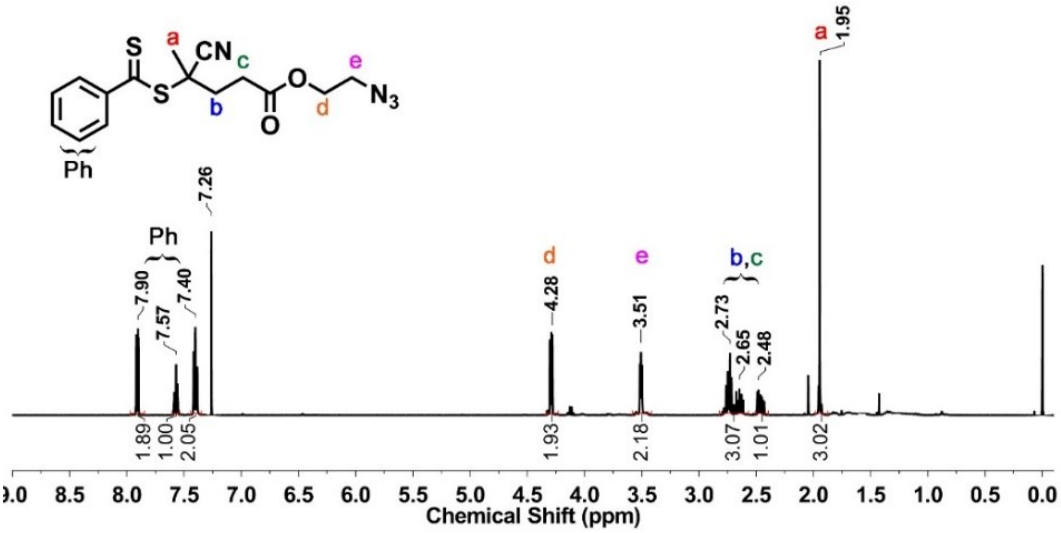

Figure S7. ^{1}H-NMR spectrum of 2-azidoethyl 4-cyano-4-((phenylcarbonothioyl)thio) pentanoate (CPADB-N_3) in $CDCl_3$ (500 MHz).

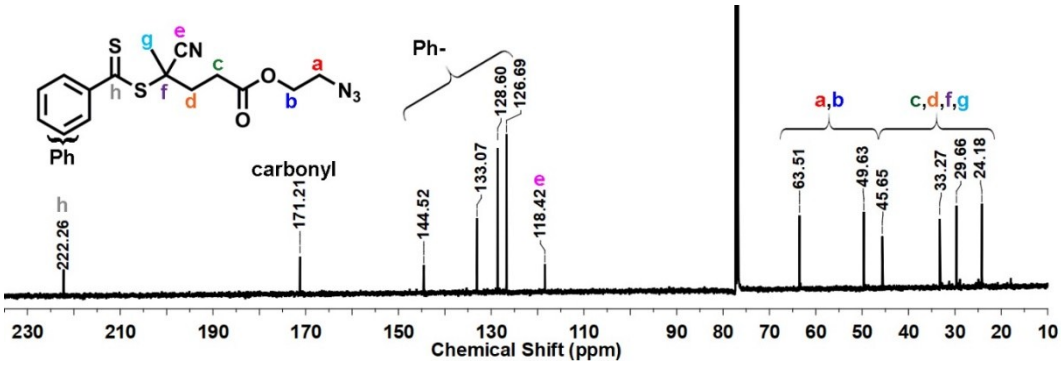

Figure S8. ^{13}C-NMR spectrum of 2-azidoethyl 4-cyano-4-((phenylcarbonothioyl)thio) pentanoate (CPADB-N_3) in $CDCl_3$ (125 MHz).

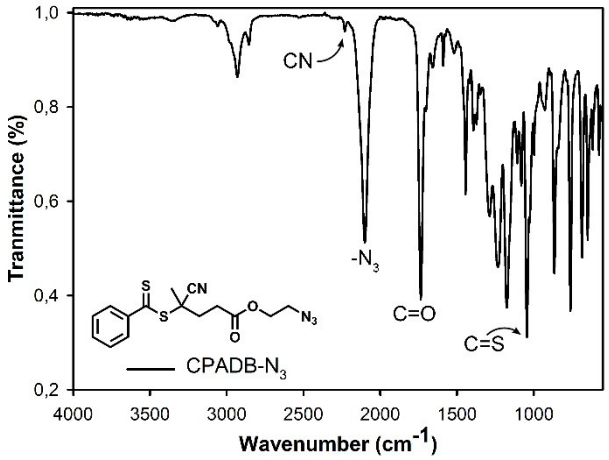

Figure S9. FT-IR spectrum of 2-azidoethyl 4-cyano-4-((phenylcarbonothioyl)thio) pentanoate (CPADB-N_3).

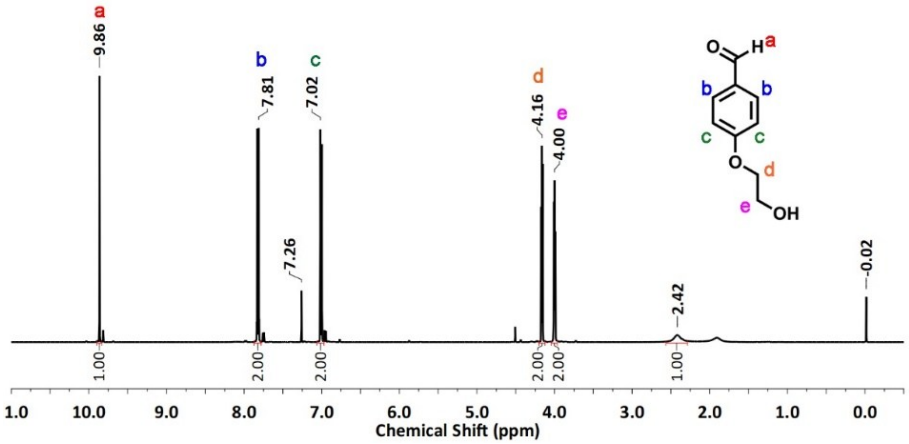

Figure S10. [1]H-NMR spectrum of *p*-(2-hydroxyethoxy)benzaldehyde (PEHBA) in $CDCl_3$ (500 MHz).

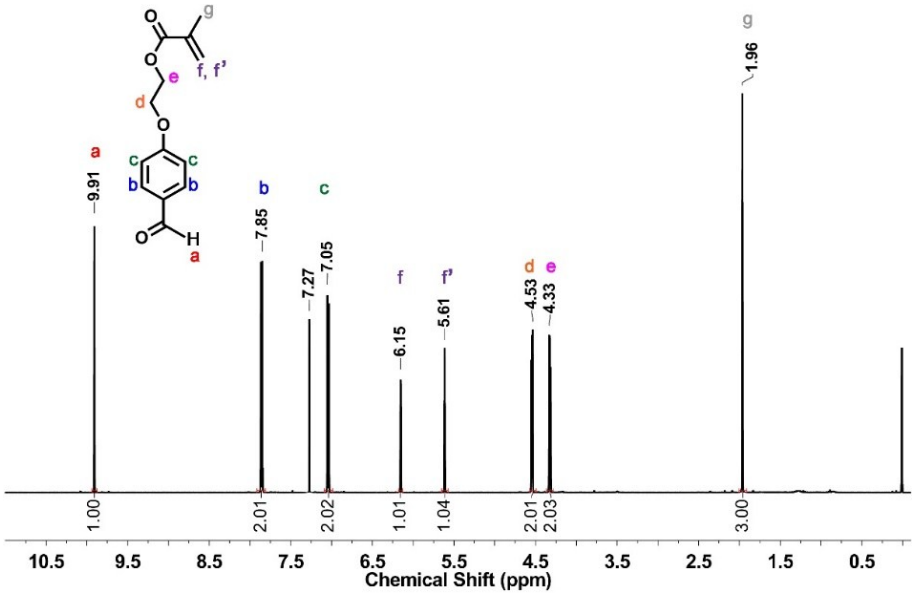

Figure S11. [1]-H NMR spectrum of p-(2-methacryloxyethoxy)benzaldehyde (MAEBA) in $CDCl_3$ (500 MHz).

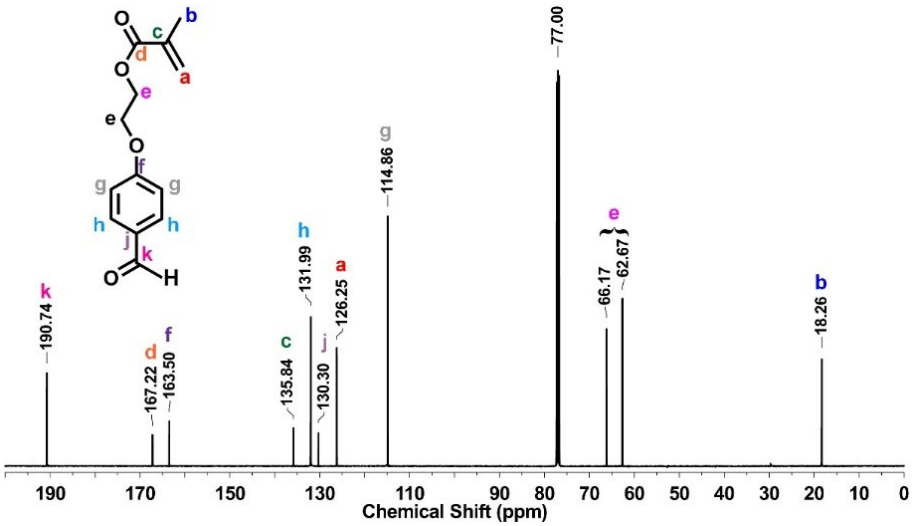

Figure S12. [13]C NMR spectrum of *p*-(2-methacryloxyethoxy)benzaldehyde (MAEBA) in $CDCl_3$ (125 MHz).

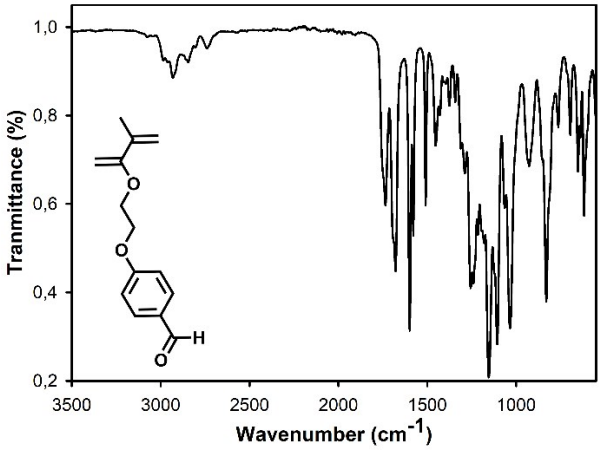

Figure S13. FT-IR spectrum of *p*-(2-methacryloxyethoxy)benzaldehyde (MAEBA).

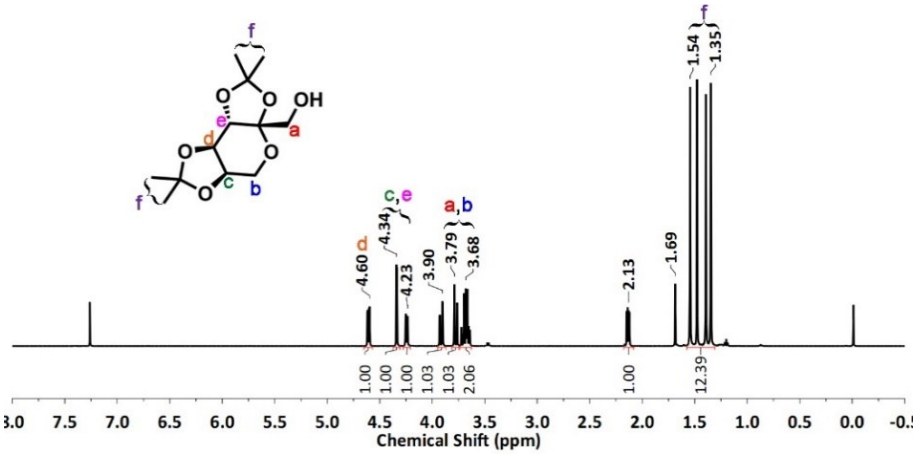

Figure S14. [1]H-NMR spectrum of 2,3:4,5 di-*O*-isopropylidene β-D-fructopyranose in $CDCl_3$ (500 MHz).

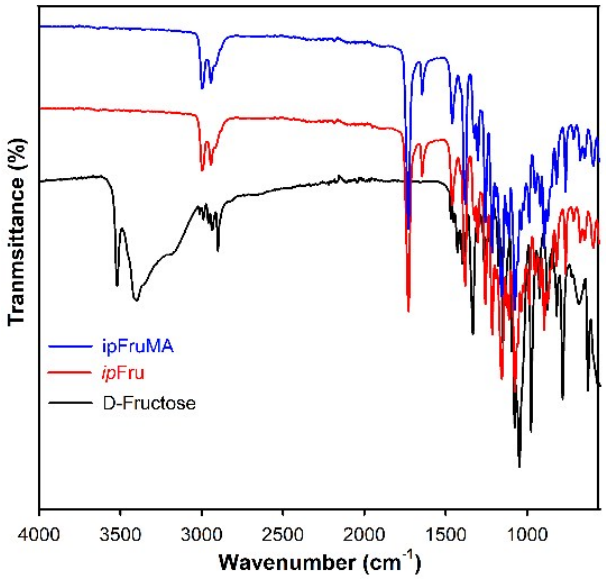

Figure S15. FT-IR spectra of D-Fructose (black), 2,3:4,5 di-*O*-isopropylidene β-D-fructopyranose (red) and 1-*O*-methacryloyl 2,3:4,5-di-*O*-isopropylidene-β-D-fructopyranose (blue).

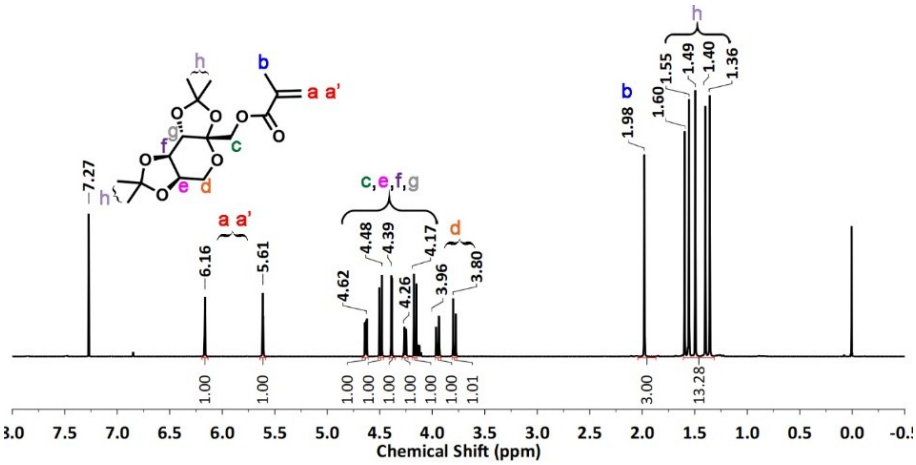

Figure S16. ^{1}H-NMR spectrum of 1-*O*-methacryloyl 2,3:4,5-di-*O*-isopropylidene-β-D-fructopyranose in $CDCl_3$ (500 MHz).

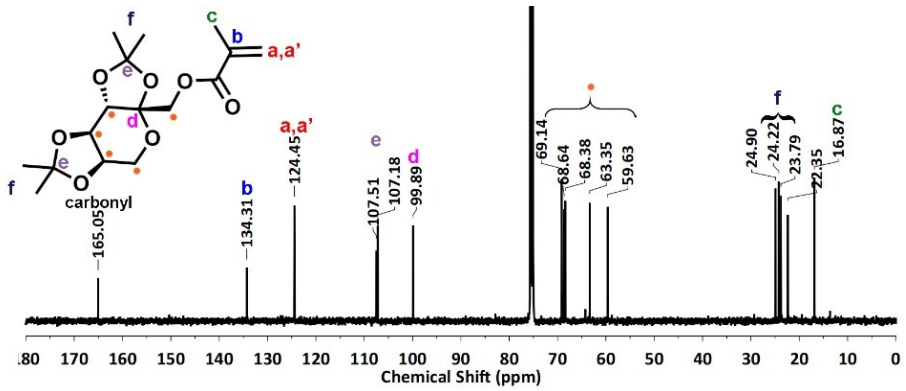

Figure S17. ^{13}C-NMR spectrum of 1-*O*-methacryloyl 2,3:4,5-di-*O*-isopropylidene-β-D-fructopyranose in $CDCl_3$ (125 MHz).

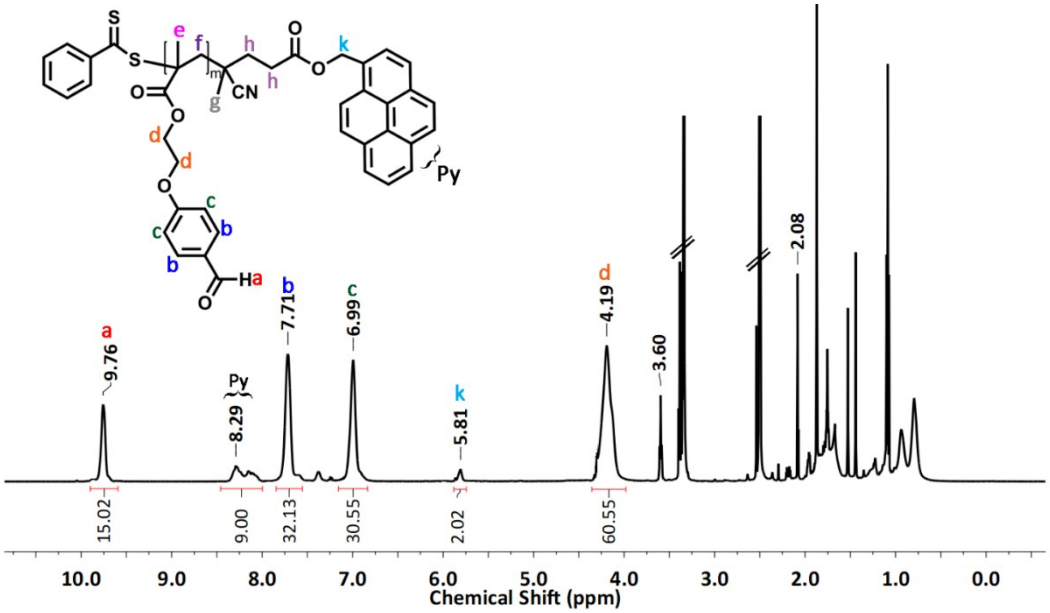

Figure S18. ^{1}H-NMR spectrum of P(MAEBA)-Py (**P1**) in $CDCl_3$ (500 MHz).

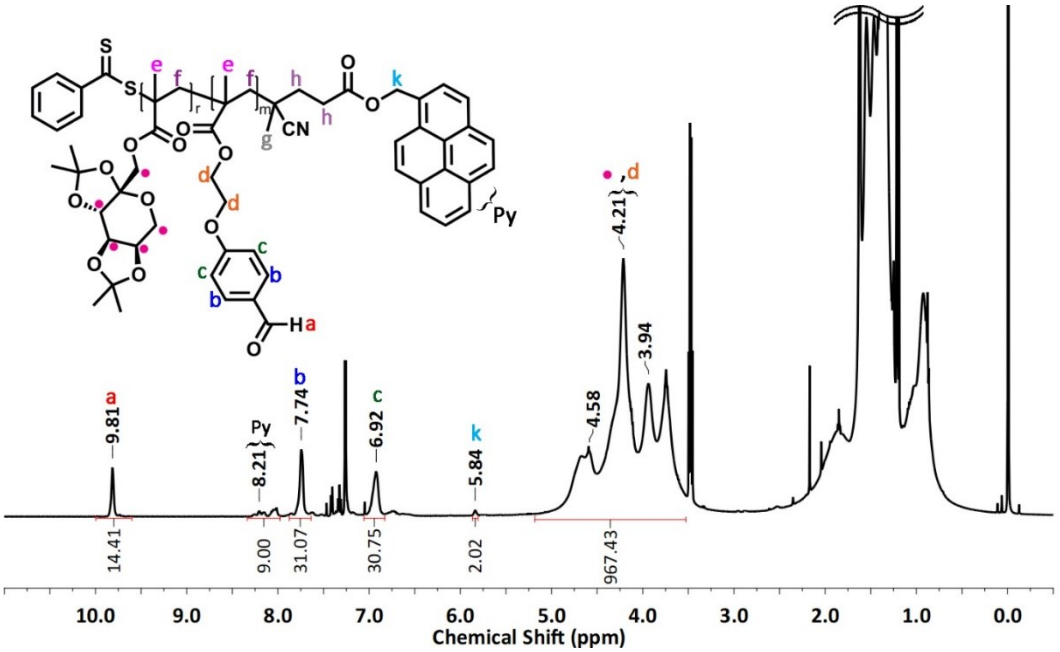

Figure S19. ^{1}H-NMR spectrum of P(*ip*FruMA-*b*-MAEBA)-Py (**P3**) in $CDCl_3$ (500 MHz).

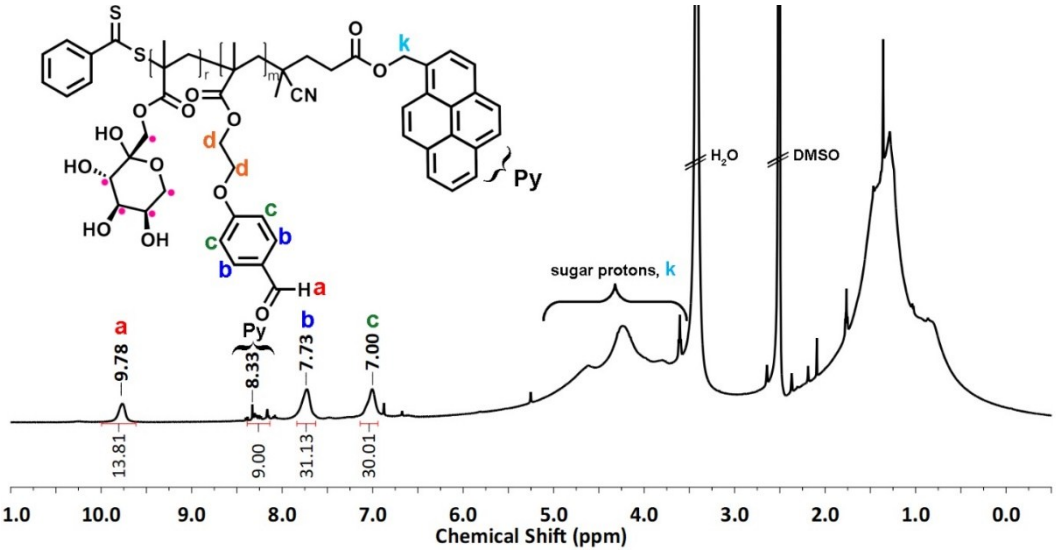

Figure S20. ^{1}H-NMR spectrum of P(FruMA-*b*-MAEBA)-Py (**P5**) in DMSO-d_6 (500 MHz).

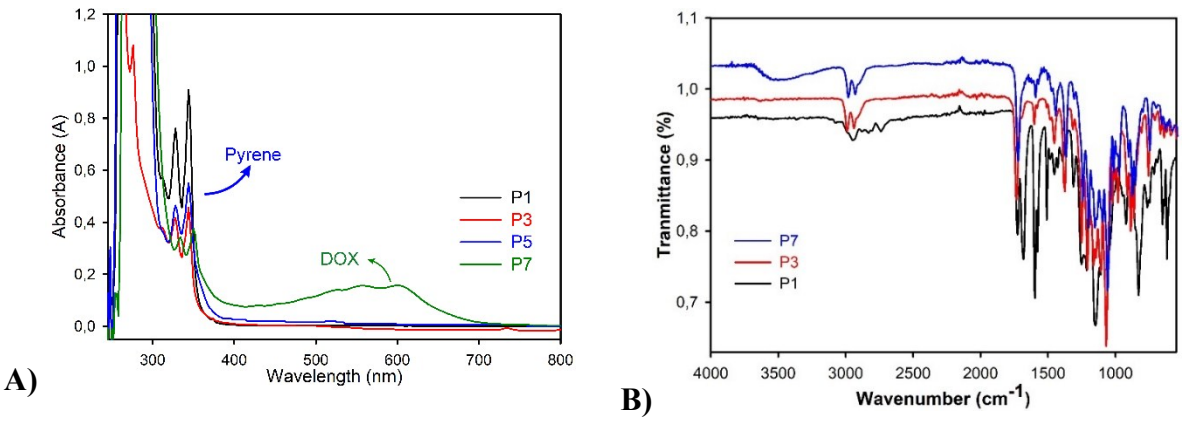

Figure S21. A) UV spectra of **P1, P3, P5** and **P7 B)** FT-IR spectra of **P1**, **P3** and **P7**.

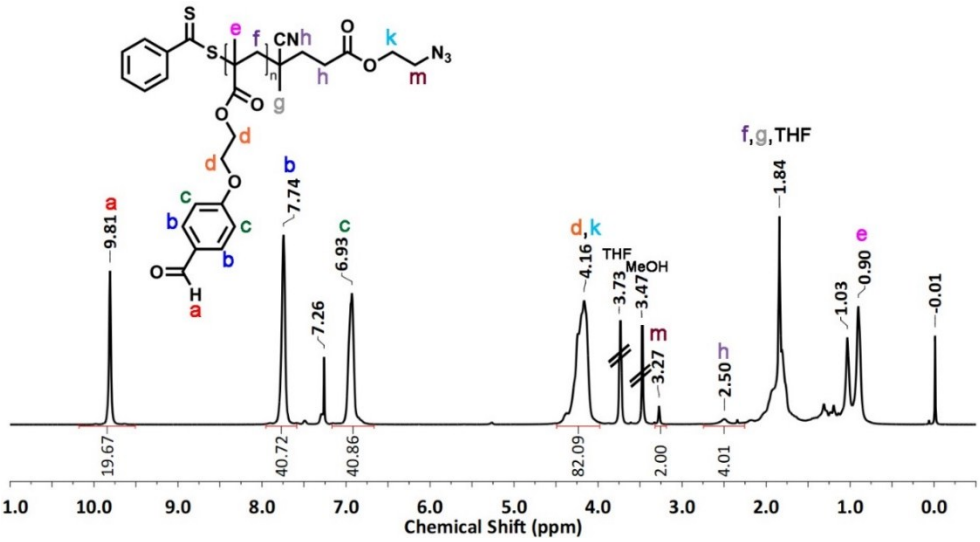

Figure S2232. ^{1}H-NMR spectrum of P(MAEBA)-N_3 (**P2**) in $CDCl_3$ (500 MHz).

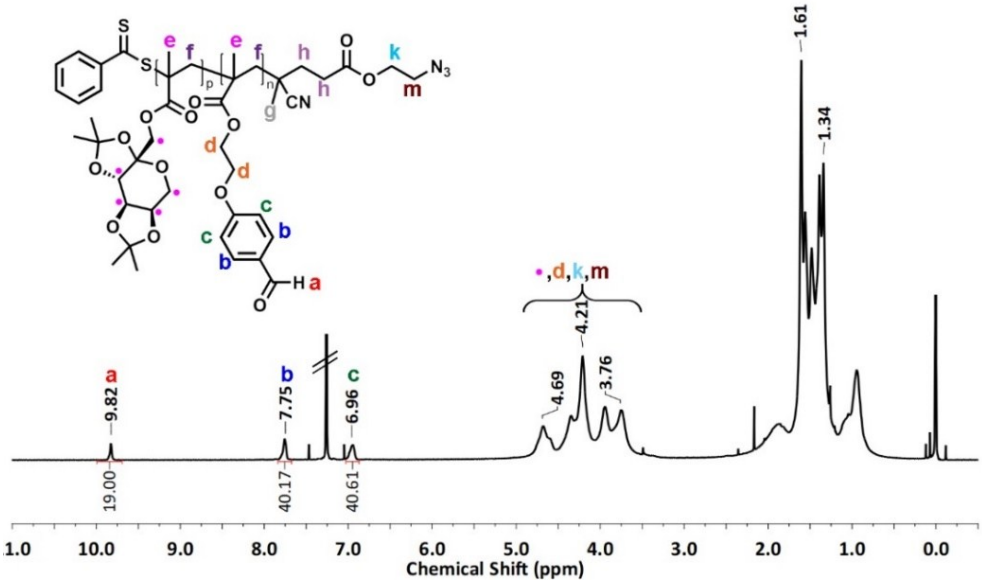

Figure S23. ^{1}H-NMR spectrum of P(*ip*FruMA-*b*-MAEBA)-N_3 (**P4**) in $CDCl_3$ (500 MHz).

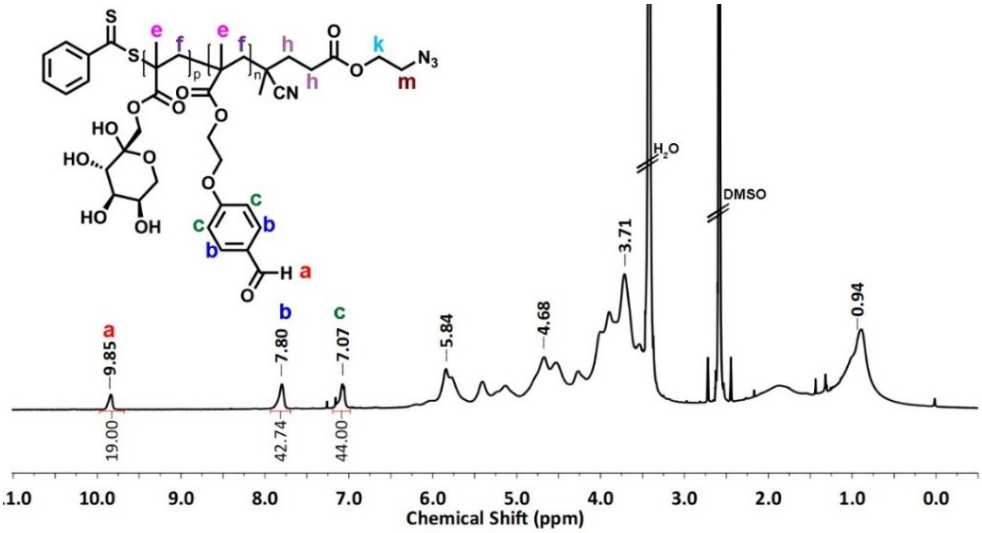

Figure S24. ^{1}H-NMR spectrum of P(FruMA-*b*-MAEBA)-N_3 (**P6**) in DMSO-d_6 (500 MHz).

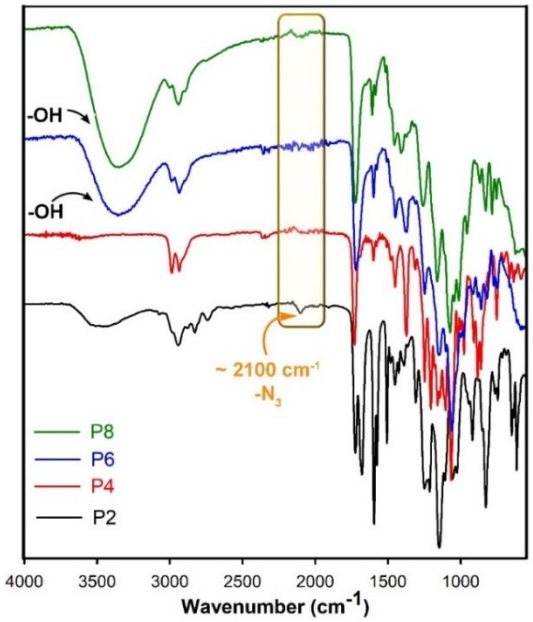

Figure S25. FT-IR spectra of **P2**, **P4**, **P6, P8**.

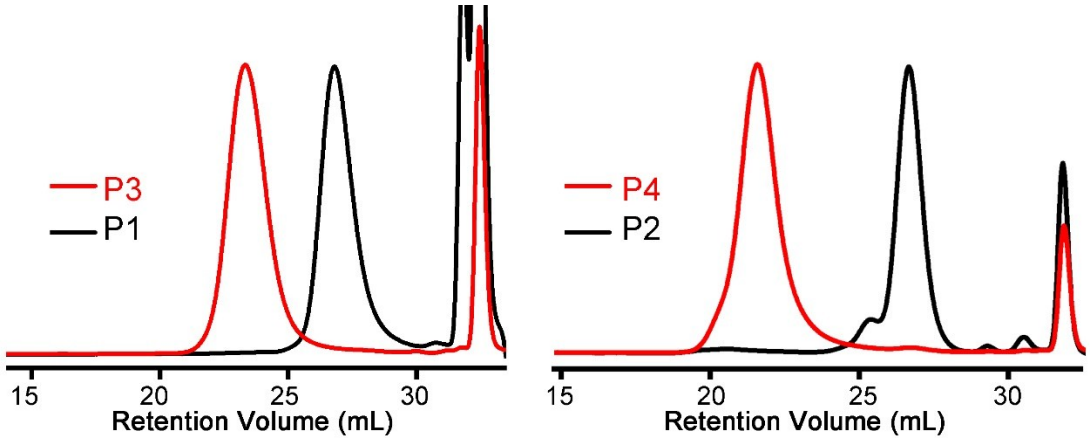

Figure S26. THF-GPC traces of **P1**-**P4**.

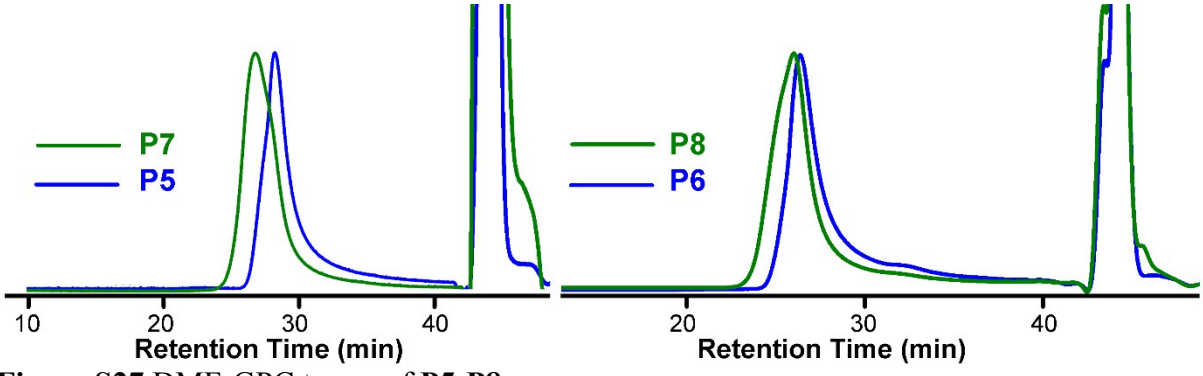

Figure S27 DMF-GPC traces of **P5**-**P8**.

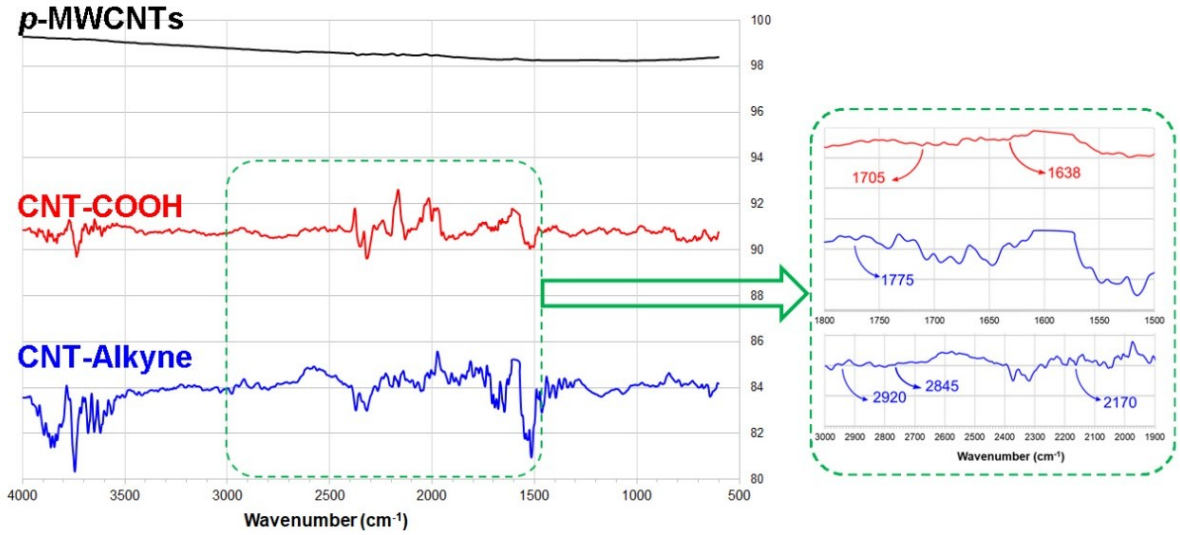

Figure S28. FT-IR spectra of ***p*-MWCNTS, CNT-COOH** and **CNT-Alkyne**.

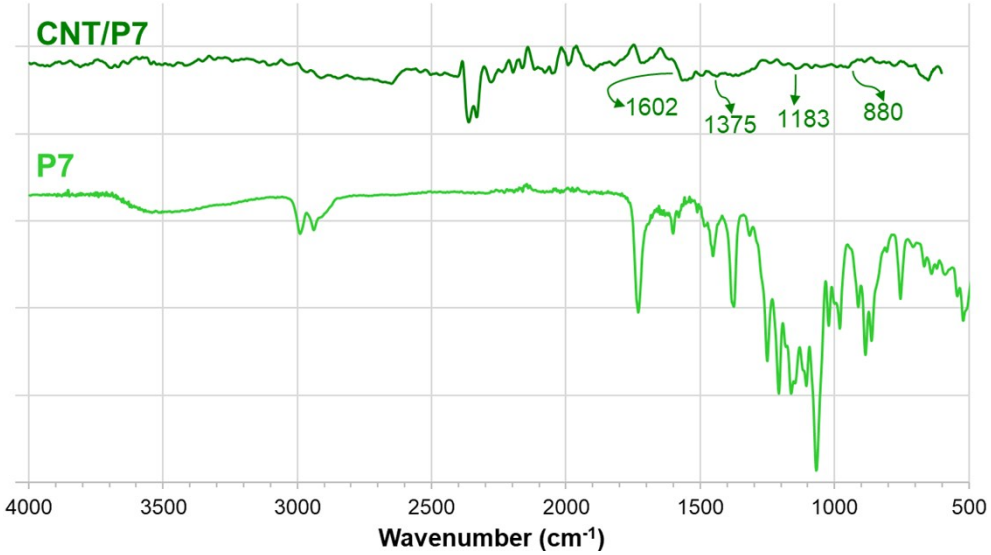

Figure S29. FT-IR spectra of **CNT/P7** and **P7**.

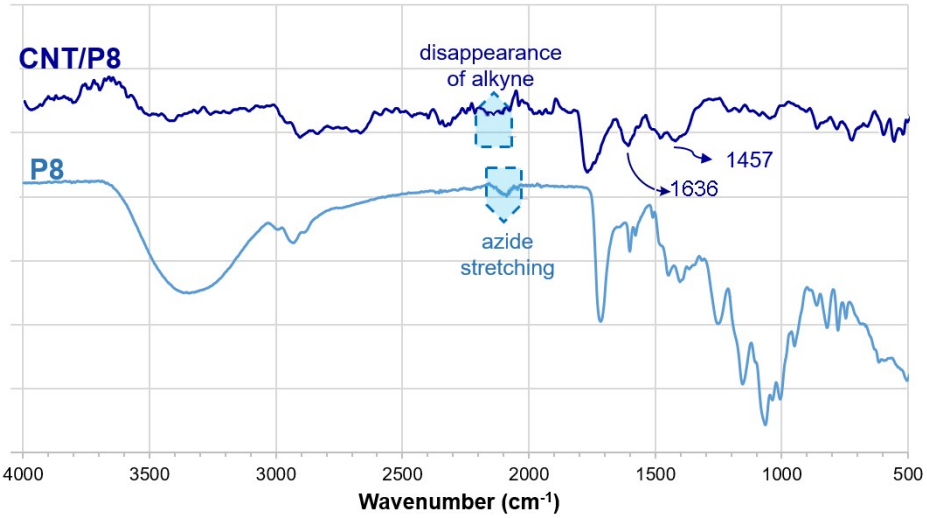

Figure S30. FT-IR spectra of **CNT/P8** and **P8**.

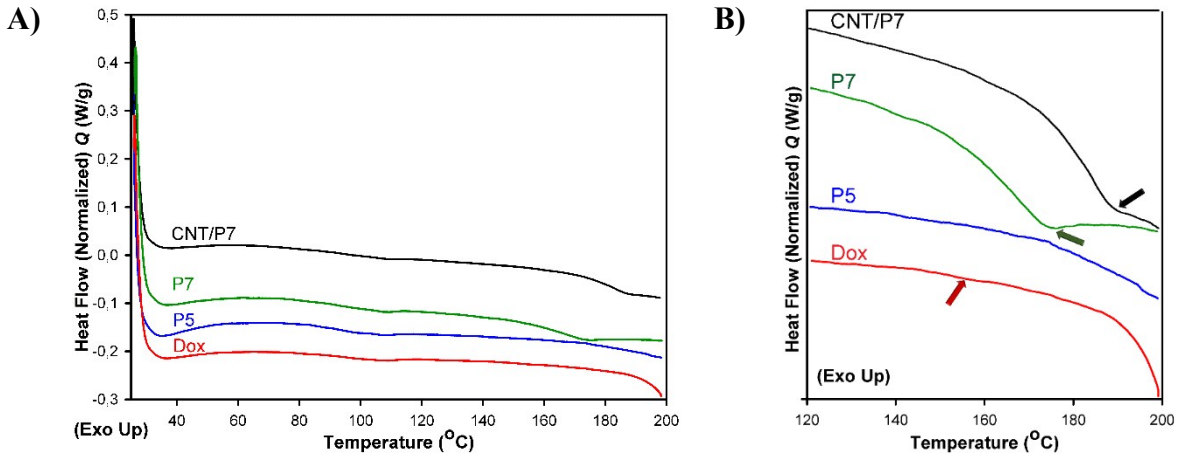

Figure S31. DSC thermogram of **Dox**, **P5**, **P7** and **CNT/P7** (second heating scan, in N_2) with a heating rate of 10 °C/min.

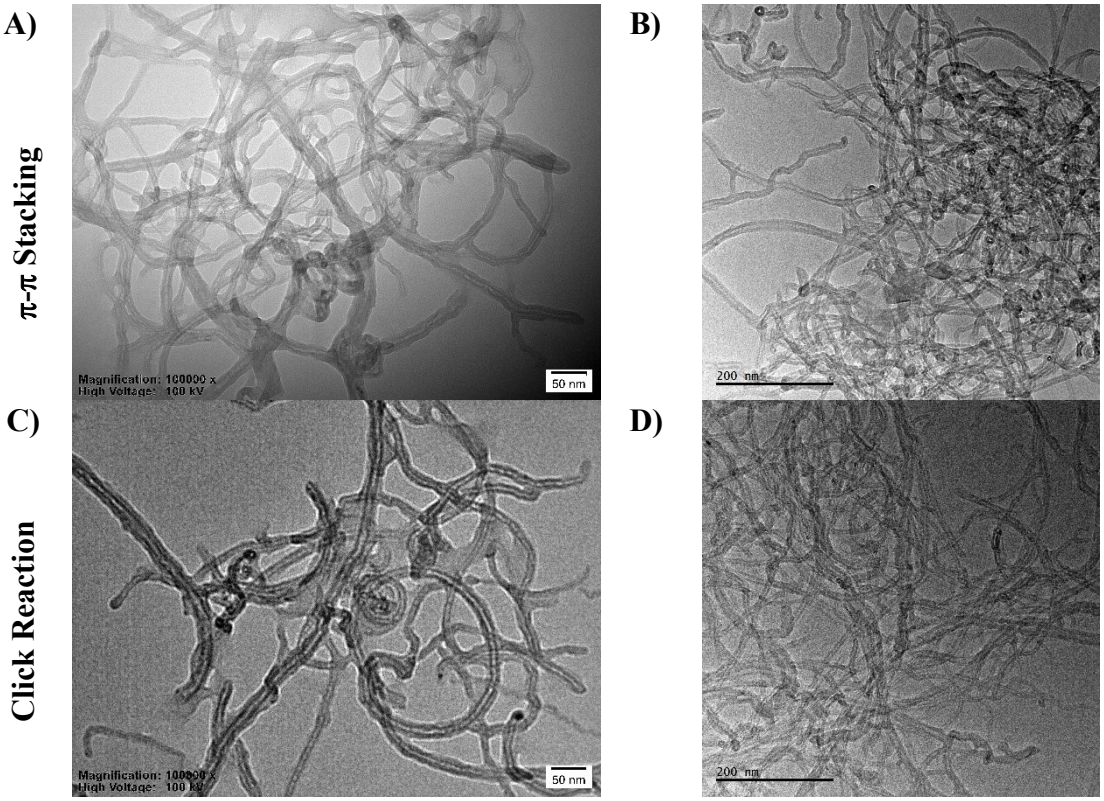

Figure S32. TEM images of **A) CNT/P7, B) CNT/P7/FA, C) CNT/P8, D) CNT/P8/FA**.

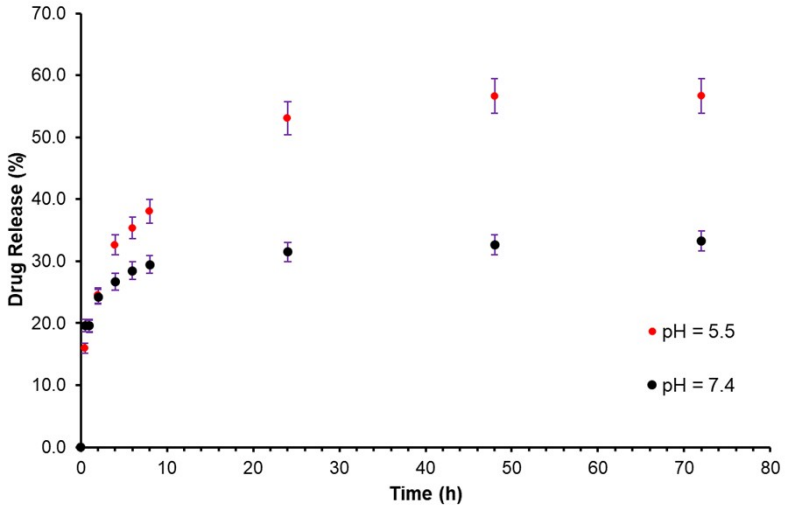

Figure S33. Release of Dox from **CNT/P7** was measured in different pH buffer solutions (pH= 5.5 and pH 7.4) by UV-Vis spectrophotometer.

A)

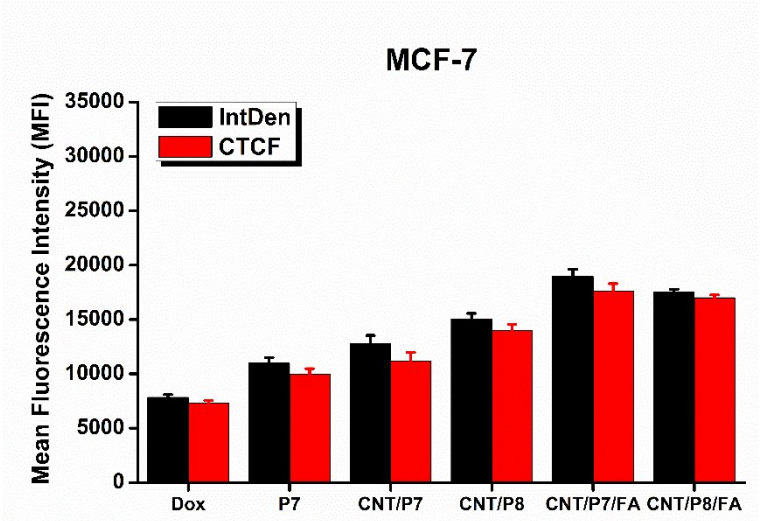

B)

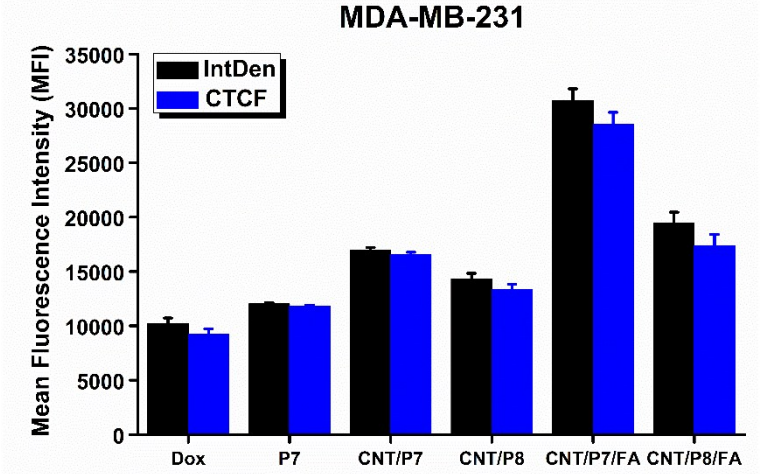

Figure S34. Mean fluorescence intensity (MFI) values determined from CLSM images. The values are means of corrected total cell fluorescence (CTCF) and integrated density (IntDen) and presented with SDs depicted by the error bars.

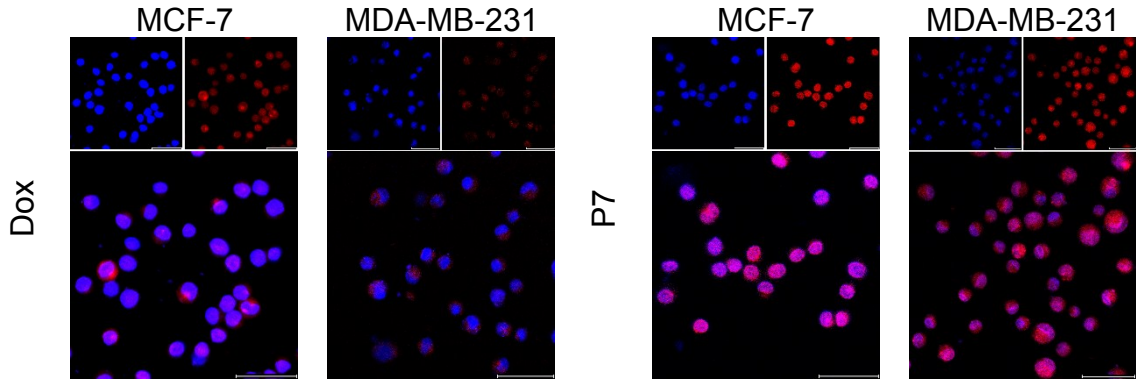

Figure S35. Cellular uptake of Dox and P7 by MCF-7 and MDA-MB-231 cells after 24 h incubation (intracellular Dox showed in red; nuclei showed in blue; and merged images). Scale bar in the all images: 50 μm.

A)

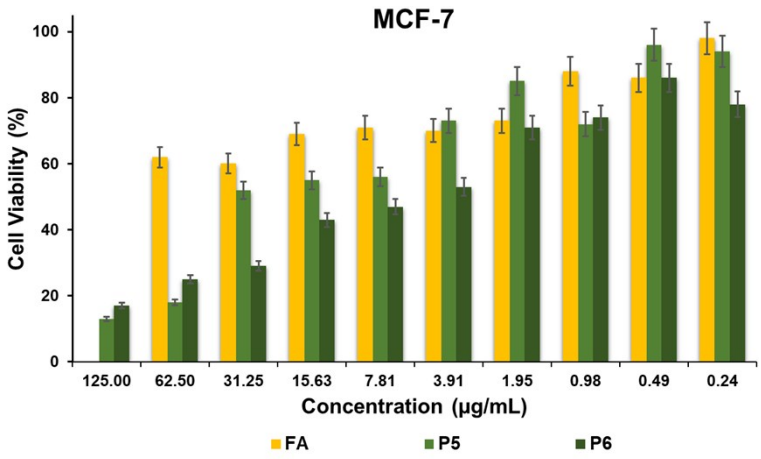

B)

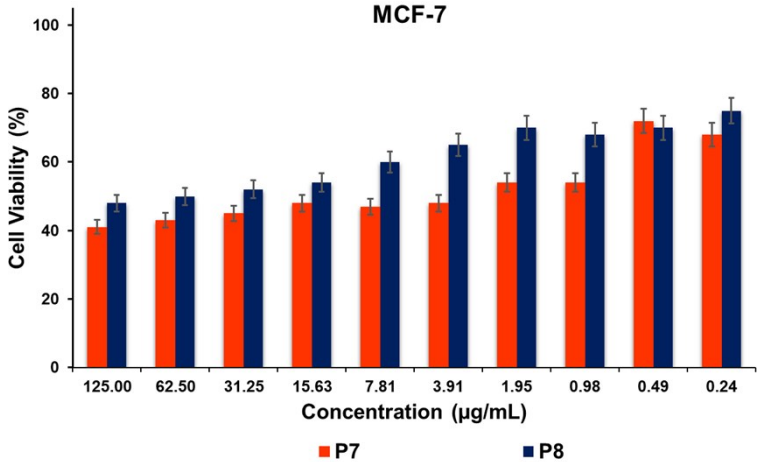

C)

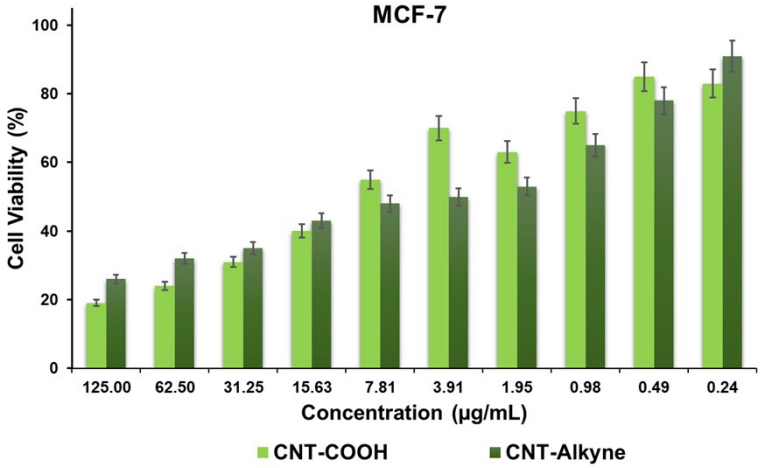

Figure S36. Cell viability (in %) after exposing a solution containing **A) FA**, **P5**, **P6**; **B) P7**, **P8** and **C) CNT-COOH**, **CNT-Alkyne** to MCF-7 cells for 24 h. Data are presented as mean ± SD.

A)

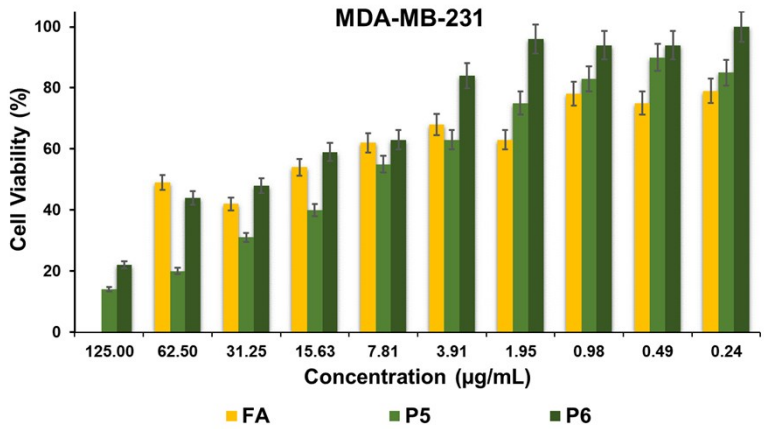

B)

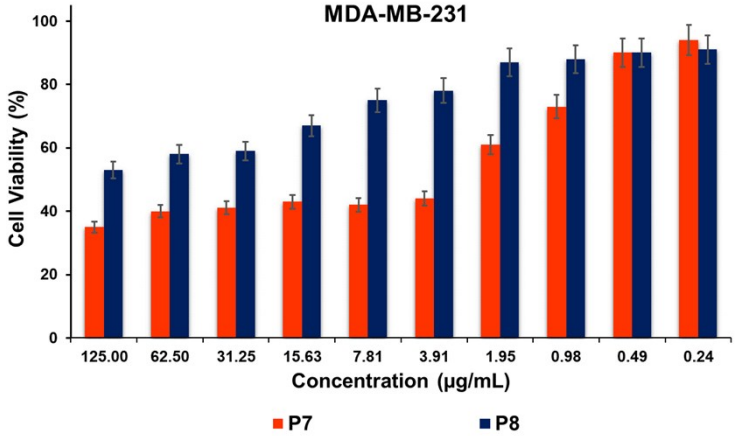

C)

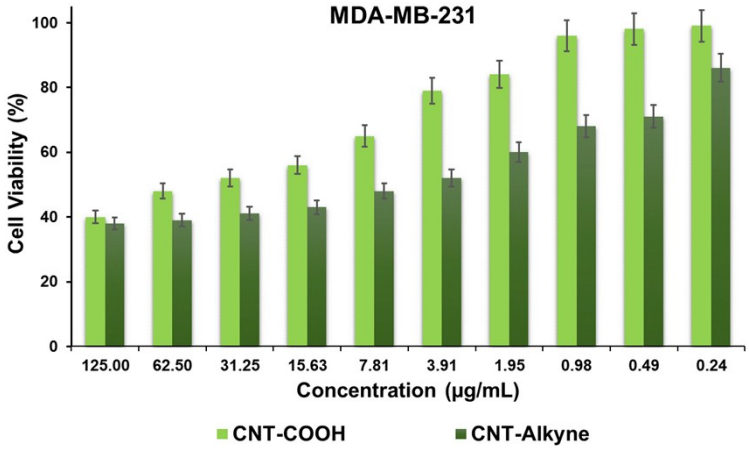

Figure S37. Cell viability (in %) after exposing a solution containing **A) FA**, **P5**, **P6**; **B) P7**, **P8** and **C) CNT-COOH**, **CNT-Alkyne** to MDA-MB-231 cells for 24 h. Data are presented as mean ± SD.

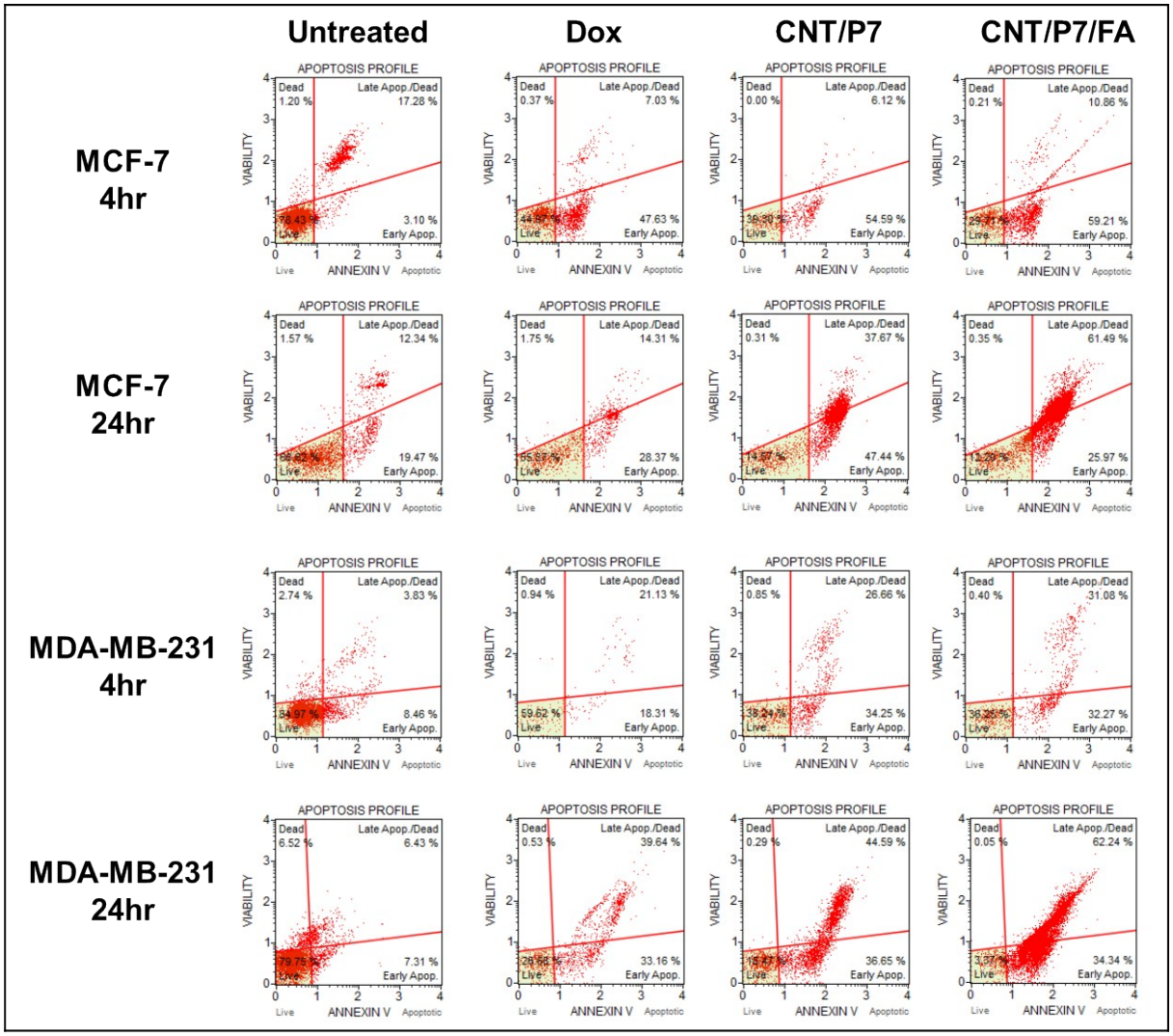

Figure S38. Apoptosis profiles for MCF-7 and MDA-MB-231 cells after **CNT/P7**, **CNT/P7/FA** and free **Dox** treatments.

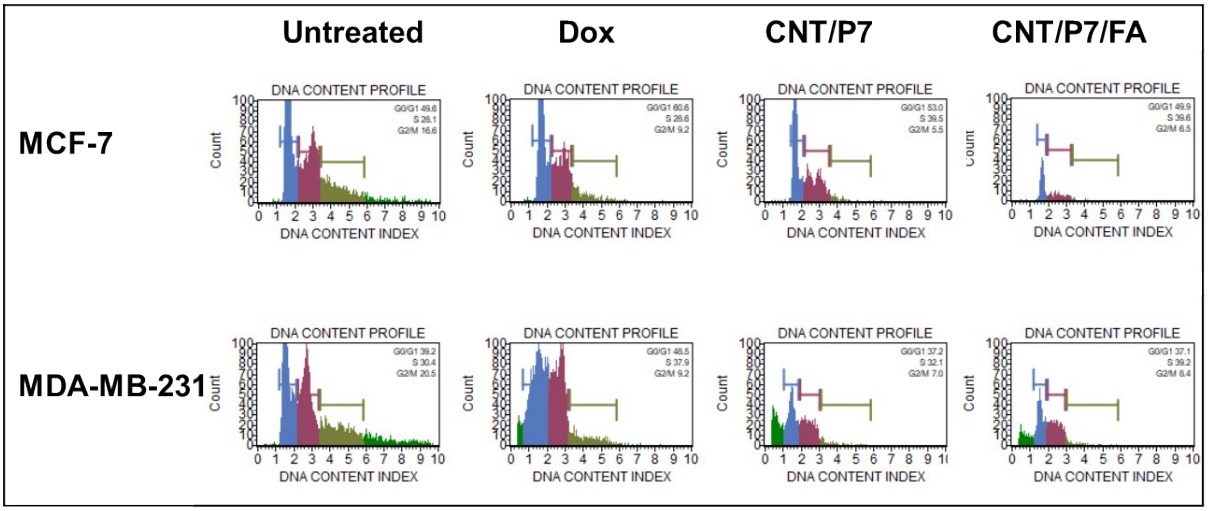

Figure S39. DNA histograms showing changes in cell cycle distributions after treatment with free **Dox**, **CNT/P7** and **CNT/P7/FA**.